Talanta 125 (2014) 221–226

Contents lists available at ScienceDirect

Talanta

journal homepage: www.elsevier.com/locate/talanta

Dopamine functionalized–CdTe quantum dots as fluorescence probes for L-histidine detection in biological fluids

Fanping Shi, Siyu Liu, Xingguang Su *

Department of Analytical Chemistry, College of Chemistry, Jilin University, Changchun 130012, China

ARTICLE INFO

Article history:
Received 29 November 2013
Received in revised form
23 February 2014
Accepted 24 February 2014
Available online 3 March 2014

Keywords:
L-Histidine
Ni^{2+}
Quantum dots
Dopamine
Fluorescence

ABSTRACT

In this paper, we developed dopamine functionalized–CdTe quantum dots as fluorescence probes for the determination of L-histidine. Firstly, CdTe was covalently linked to dopamine to form a kind of fluorescence sensor with pyrocatechol structure on the surface. The photoluminescence intensity of CdTe–dopamine (QDs–DA) could be quenched by Ni^{2+} due to the strong coordination interaction between the pyrocatechol structure of QDs–DA and Ni^{2+}. In the presence of L-histidine, Ni^{2+} preferred to bind with L-histidine due to high affinity of Ni^{2+} to L-histidine and the photoluminescence intensity of QDs–DA was recovered. The recovered photoluminescence intensity of QDs–DA was proportional to the concentration of L-histidine in the ranges of 1.0×10^{-6}–1.0×10^{-4} mol L^{-1} and the detection limit was 5.0×10^{-7} mol L^{-1} respectively. The established method showed a good selectivity for L-histidine among other common amino acids, and it was applied for determination of L-histidine in human serum sample with satisfactory results.

1. Introduction

L-Histidine (L-his), an essential amino acid in humans and other mammals, has caused wide concern in the area of biochemistry due to its very active role in many biological systems. L-His is a basic, genetically coded natural amino acid. The imidazole side chain of L-his acts as a common coordinating ligand in metalloproteins which controls the transmission of metal elements in biological bases. As a neurotransmitter or neuromodulator, it performs significant functions in the central nervous system of mammals, such as the generation of retina [1–3]. L-Histidine-rich proteins are found to play many important roles in humans. Friedreich ataxia, epilepsy, Parkinson's disease, and the failure of normal erythropoiesis development are all a result of the abnormal situation of L-his [4,5]. Recent researches have also shown that the impaired nutritional state of patients with chronic kidney disease could be attributed to the deficiency of L-his [6]. Therefore, the detection of L-his in biological fluids has important implications in the area of biochemistry systems. Several methods have been developed for the detection of L-his, including high performance liquid chromatography (HPLC) [7,8], capillary electrophoresis (CE) [9], voltammetry [10], mass spectrometry [11], and spectrophotometry [12,13]. Although these methods are mature enough to be systematic, inevitably there are some shortcomings such as complicated sample pre-preparation, long-time consuming operation procedures, expensive instrumentation, chemical modifications, etc. These limits urge us to explore more novel methods for L-his detection.

Quantum dots (QDs), as a new class of fluorescent probes, have attracted considerable attention in recent years. Compared with conventional organic fluorescent dyes, QDs have many unique optical properties, like strong signal intensity, high quantum yield, tunable size-dependent photoluminescence and narrow emission peaks, which gained them increased attention in many fields [14]. The application of QDs in biological fields such as fluorescence imaging of cells and tissues has already made great progress [15,16]. Furthermore, surface-functionalized quantum dots are widely used as fluorescent labels for sensing and biosensing events as well. The surface of QDs has been engineered with ligands featuring diverse affinity and specificity towards a multitude of target analytes, which may participate in the subsequent attachment of other biomolecules, and specific detections are made possible [17–19].

Dopamine is released by nerve cells to send signals to other nerve cells. As an important catecholamine neurotransmitter, it helps control the brain's reward and pleasure centers while also regulating movement and emotional responses [20,21]. In this work, we utilized dopamine to functionalize CdTe QDs. Amino groups of dopamine are available for the amide formation with carboxylic acid groups capping CdTe QD, which allow dopamine to link to the surface of QDs with 1-ethyl-3-[3-dimethylaminopropyl] carbodiimide hydrochloride (EDC) and N-hydroxysuccinimide

* Corresponding author. Tel.: +86 431 85168352.
E-mail address: suxg@jlu.edu.cn (X. Su).

http://dx.doi.org/10.1016/j.talanta.2014.02.060
0039-9140

(NHS) as cross-linking agents. Recently, some researches about quantum dots–dopamine conjugation (QDs–DA) have been reported. Clarke reported the photo-physics characters of dopamine-modified quantum dots and its effects on biological systems in 2006 [22]. They continued their research on quantifying photo-enhancement and photo-bleaching on a single particle and the behavior of QDs–DA in living cells in 2007 [23], and its lifetime and photoluminescence intensities were also investigated in 2009 [24].

Recently, Ni^{2+}–histidine affinity pair has been widely used for the separation, purification and tracking of histidine-containing peptides and histidine-tagged proteins. The specific interaction between Ni^{2+} and L-histidine was accomplished through the coordination of Ni^{2+} and the imidazole residue as well as the primary amine and/or carboxylic groups of histidine [25–28]. Here we develop a novel fluorescence probe for L-his detection based on the QDs–DA and the affinity pair mentioned above. In this work, dopamine was linked to the surface of 3-mercaptopropionic acid (MPA)-capped CdTe QDs via a cross-linking reaction. The dopamine-functionalized–CdTe QDs had a stable, symmetric fluorescence emission centered at 568 nm. The pyrocatechol structure on the surface of QDs–DA could coordinate with Ni^{2+}. This combination led to the fluorescence quenching of QDs–DA via electron transfer. In the presence of L-his, the photoluminescence (PL) intensity of QDs–DA is recovered due to the high affinity of Ni^{2+} to L-his. Thus, a simple and fast fluorescence turn-on sensor is constructed and it offers good selectivity for L-his over other amino acids.

2. Experimental

2.1. Materials

All chemical reagents were of analytical grade and used without further purification. The water used in all experiments has a resistivity higher than 18 MΩ cm^{-1}. Mercaptopropionic acid (MPA) (99%) was purchased from J&K Chemical Co. and tellurium powder (~200 mesh, 99.8%), $CdCl_2$ (99%), $NaBH_4$ (99%), 1-ethyl-3-[3–dimethylaminopropyl] carbodiimide hydrochloride (EDC), N-hydroxysuccinimide (NHS), and dopamine (DA) were purchased from Sigma-Aldrich Corporation. NaCl, KCl, $Ca(NO_3)_2$, $Mg(NO_3)_2$, $Ba(NO_3)_2$, beta-cyclodextrin, glucose, sodium tartrate, arginine, tyrosine, glycin, phenylalanine, cystine, asparagic acid and lysine were purchased from Beijing Dingguo Biotechnology Co. Ltd. All the modifiers were prepared with 5 mmol L^{-1} Tris–HCl buffer solution (pH=8.6). The above solutions were all stored at 0–4 °C and diluted with ultrapure water to the concentrations used in the experiment.

2.2. Instrument

All fluorescence measurements were carried out in a 1 cm path length quartz cuvette with a Shimadzu RF-5301 PC spectrofluorophotometer equipped with a xenon lamp using right-angle geometry. The excitation wavelength was 400 nm and the PL referred to the maximum emission of QDs–DA at 568 nm. UV–vis absorption spectra were obtained using a Varian GBC Cintra 10e UV–vis spectrometer. FT-IR spectra were recorded with a Bruker IFS66V FT-IR spectrometer equipped with a DGTS detector (32 scans). All the optical measurements were carried out at room temperature in ambient conditions. Transmission electron microscopy (TEM) images were obtained with a JEOL-3010 electron microscope operating at 300 kV. TEM samples were prepared by dropping the aqueous QDs–DA solution onto carbon-coated copper grids and allowing the excess solvent to evaporate. All pH measurements were made with a Starter-2C pH meter obtained from Ohaus Instruments Co. Ltd., Shanghai, China.

2.3. Preparation of MPA-capped CdTe QDs

Synthesis of mercaptopropionic acid (MPA)-capped CdTe QDs in this study was carried out according to the previous report [29]. Briefly, the precursor solution of CdTe QDs was formed in water by adding fresh NaHTe solution to 1.25×10^{-3} mol L^{-1} N_2-saturated $CdCl_2$ solution at pH 11.2 in the presence of MPA as a stabilizing agent. The molar ratio of Cd^{2+}/MPA/HTe^- was charged at 1:2.4:0.5. The CdTe precursor solution was subjected to reflux at 100 °C in open-air conditions with a condenser attached and different sizes of CdTe QDs were obtained at different refluxing times. Ethanol was added to the stock solution to obtain CdTe QDs precipitate and the process was repeated three times. The unreacted residues were removed by the cycled washing. The purified CdTe QDs were dissolved in PBS buffer (0.1 mol L^{-1}, pH=7.4), and stored in a darkroom. The photo-luminescence emission wavelength of CdTe QDs used in the present experiments was 570 nm and the concentration of QDs was 1×10^{-6} mol L^{-1}.

2.4. Preparation of dopamine-functionalized–CdTe QDs

The conjugation of dopamine to CdTe QDs was performed utilizing EDC and NHS as coupling reagents according to previous reports [22,29]. Briefly, the CdTe QDs solution was mixed with EDC and NHS at room temperature and then dopamine was added into the solution and stirred for more than three hours (the mole ratio of QD to NHS, EDC, dopamine was 1:1500:1500:1000). The obtained QDs–DA was purified by precipitation with addition of ethanol to the reaction system, and the purified QDs–DA powder was dissolved in aqueous solution and stored in a darkroom.

2.5. Detection process

To study the fluorescence quenching effect of Ni^{2+} on the QDs–DA, 50 μL QDs–DA solution, 100 μL of 0.1 mol L^{-1} Tris–HCl buffer solution and different concentrations of Ni^{2+} solution were successively added into a 2 mL calibrated test tube and then diluted to the mark with deionized water shaken thoroughly until the solution was fully mixed.

To study the effect of L-his on the fluorescence restoration of QDs–DA–Ni (II) system, 50 μL QDs–DA, 100 μL of 0.1 mol L^{-1} Tris–HCl buffer solution, a certain volume of Ni^{2+} and different concentrations of L-his solution were successively added into a 2 mL calibrated test tube and diluted to the mark with deionized water, then shaken thoroughly until the solution was fully mixed. In the experiments, all the PL measurements were performed under the same conditions: the slit widths of the excitation and emission were both 10 nm and the excitation wavelength was set at 400 nm. The PL intensities were recorded in the wavelength range of 480–680 nm.

2.6. Human serum samples detection

For serum samples detection, drug-free human blood samples were collected from healthy volunteers at the Hospital of Changchun China–Japan Union Hospital. All the blood samples were obtained by venipuncture and centrifuged at 10,000 rpm for 10 min at room temperature. Due to the high protein bonding in the blood plasma, some pretreatments were carried out to eliminate the interferences and improve the recovery according to previous reports [30,31]. The supernatant in the samples was separated and deproteinized by adding acetonitrile (CH_3CN: serum=1:1). After vigorously shaking for 2 min, the mixture was

centrifuged at 10,000 rpm for 10 min at 4 °C. The obtained supernatant was filtered two times. The filtrate was adjusted to neutral pH and then diluted by 50 times with deionized water. Different concentrations of L-his were added to the diluted serum samples to prepare the spiked samples. Real samples detection was carried out using the procedure described above.

3. Results and discussion

3.1. Spectral characterization of dopamine-functionalized–CdTe QDs (QDs–DA)

In this study, CdTe QDs were synthesized by refluxing routes and then dopamine molecules were linked to the surface of CdTe QDs as shown in Scheme 1. The fluorescence emission and UV–vis absorption spectra of CdTe QDs and QDs–DA are shown in Fig. 1A. It can be seen that the fluorescence emission peak of MPA-capped CdTe QDs at 570 nm is narrow and symmetrical, and the UV–vis absorption peak is around 490 nm. After the dopamine was linked to the surface, MPA-capped CdTe was changed from negatively charged acetate to electron-rich phenol, and the fluorescence emission peak of QDs–DA exhibited a blueshift. Fig. 1B shows the TEM micrograph of CdTe QDs–DA. It can be seen that the size distribution of CdTe QDs–DA was reasonably uniform and the particle size of most CdTe QDs–DA was approximately 2 nm.

Fig. 1C shows the FT-IR spectra of the MPA-capped CdTe QDs (curve a) and QDs–DA (curve b). As seen in curve (a), the majority of MPA functional groups could be clearly found through the C=O stretching peak (1730 cm^{-1}) and C–H stretching peaks (2850 cm^{-1}, 2920 cm^{-1}, 2960 cm^{-1}). The characteristic peak of S–H did not appear within 2550–2680 cm^{-1}, which might be caused by the covalent bonds between thiols and metal. As seen in curve (b) the amide I band (1660 cm^{-1}) and amide II (1540 cm^{-1}) band for –CONH group appeared which was due to the conjugation of DA to the MPA-capped CdTe QDs.

3.2. Fluorescence quenching and recovery of QDs–DA with Ni (II) and L-his

In this work, we investigated the fluorescence quenching of QDs–DA induced by Ni^{2+} systematically. Fig. 2 shows the photoluminescence emission spectra of QDs–DA, QDs–DA–Ni (II), and QDs–DA–Ni (II)-His system. After the addition of 50 μmol L^{-1} Ni^{2+} the PL intensity of QDs–DA decreased to about 46.7% of the original PL intensity. When 75 μmol L^{-1} L-his was added into the QDs–DA–Ni (II) system, the PL intensity increased significantly.

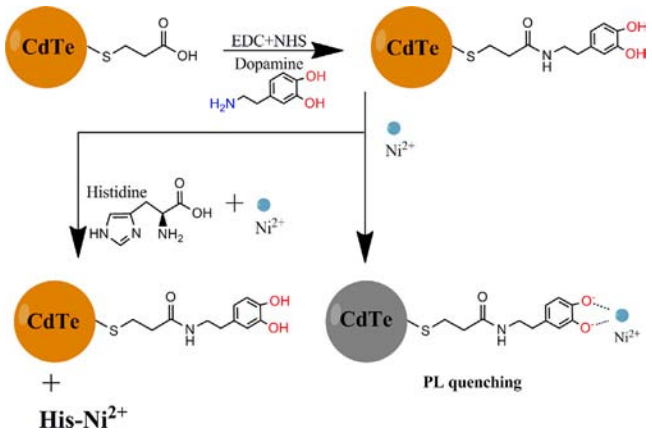

Scheme 1. Illustration of the mechanism of this novel fluorescence probe for the detection of L-histidine based on the quenching and recovery of the photoluminescence of dopamine functionalized QDs.

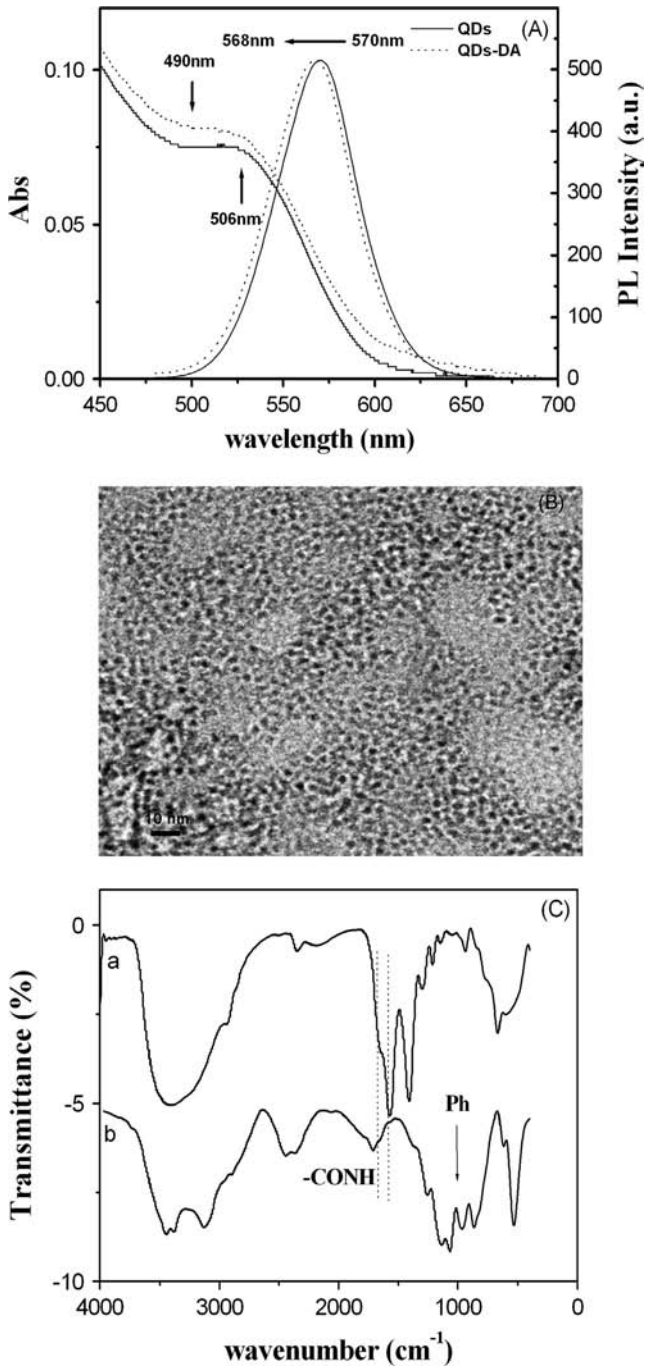

Fig. 1. (A) Normalized photoluminescence emission spectra and UV–vis spectra of QDs–DA and CdTe QDs, (B) TEM images of QDs–DA nanoparticles, and (C) FT-IR spectra of the MPA-capped CdTe QDs (curve a) and QDs–DA (curve b).

The fluorescence change tends to be slow after incubation for 10 min. So in further experiments, both the QDs–DA–Ni (II) system and QDs–DA–Ni (II)-His system were shaken thoroughly for 10 min, and then the PL intensities of the mixtures were recorded. The inset shows the obvious color changes of QDs–DA (a), QDs–DA–Ni (II) system (b) and QDs–DA–Ni (II)-His system (c) under UV light (365 nm).

The pH value did not only affect the PL intensity of the original QDs–DA solution, but also the subsequent fluorescence quenching by Ni^{2+} and fluorescence recovery by L-his. We systematically discussed the pH effect on the quenched PL intensity by Ni (II) and the recovered PL intensity by L-his. As shown in Fig. 3, with increase of pH value, the PL intensity of QDs–DA solution increased

initially and reached a maximum at pH 8.2, then decreased gradually from pH 8.6 to 9.0. When 50 μmol L^{-1} Ni^{2+} was added into the QDs–DA solution, the quench effect was not very obvious in the pH range of 7.0–8.2 and the restore efficiency was modest in the presence of L-his (100 μmol L^{-1}). When the pH was 8.6, both the quench efficiency of Ni^{2+} and the restore efficiency of L-his were satisfactory. Therefore, in order to minimize distractions and obtain a better recovering condition, pH 8.6 was chosen in the further experiments.

In order to investigate the quenching ability of Ni^{2+} on the PL intensity of QDs–DA, the fluorescence spectra of QDs–DA in the presence of a series of Ni^{2+} concentrations were recorded and the results are shown in Fig. 4. It can be seen that the PL intensity of QDs–DA reduced gradually with the increasing concentration of Ni^{2+} (from 0.5 to 100 μmol L^{-1}) and there was no obvious change of spectral shape. The inset reveals the fluorescence intensity ratio I/I_0 of QDs–DA (I_0 and I are the PL intensities of QDs–DA with or without Ni^{2+}) and the Ni^{2+} concentration shows a good linear relationship in the range of 5.0×10^{-7}–5.0×10^{-5} mol L^{-1} and 5.0×10^{-5}–1.0×10^{-4} mol L^{-1}.

The linear regression equation was as follows

$I/I_0 = 0.9725 - 0.00995\left[Ni^{2+}\right]$ (μmol L^{-1}) for 5.0×10^{-7}–5.0×10^{-5} mol L^{-1} Ni^{2+} and $I/I_0 = 0.614 - 0.00231\left[Ni^{2+}\right]$ (μmol L^{-1}) for 5.0×10^{-5}–1.0×10^{-4} mol L^{-1} Ni^{2+}. The correlation coefficients were $R^2=0.9926$ and $R^2=0.9924$, respectively. The limit of detection (LOD) was found to be 0.33 μmol L^{-1} using the criterion of three times the standard deviation of the blank signal.

In the presence of L-his, the Ni (II)–L-his complex could be formed due to the high affinity of Ni^{2+} to L-his [32,33]. The quenched fluorescence of QDs–DA–Ni (II) system can be restored in the presence of L-his. We compared the quenching efficiencies of seven other transition metal ions (Mn^{2+}, Fe^{3+}, Co^{2+}, Cu^{2+}, Zn^{2+}, Cd^{2+} and Hg^{2+}) with Ni^{2+} and their restore efficiencies after addition of L-his (Fig. S1). It can be seen that Mn^{2+} and Zn^{2+} had no quenching effect on QDs–DA, while the restore efficiencies of others were far from perfect. The results showed that even the quenching effect of Ni^{2+} to QDs–DA was not the best, the restore efficiency of Ni^{2+}–histidine is much higher than other transition metal ions, which indicated that Ni^{2+}–histidine system is the most suitable pair for the determination of L-his. This makes this reaction selective for Ni^{2+} over other transition metal ions. As indicated in Fig. 5, the addition of a series of increasing concentrations of L-his resulted in the gradual enhancement of the PL intensity of the QDs–DA–Ni (II) system. From the inset we can find that the linear relationships between the fluorescence intensity ratio I_r/I_0 (I_0 is the fluorescence intensity of QDs–DA and I_r is the fluorescence intensity of QDs–DA–Ni^{2+} in the presence of the L-his) and L- his concentration could be described as follows

$I_r/I_0 = 0.47098 + 0.00241$[His](μmol L^{-1}) for 0–10 μmol L^{-1} L-his and $I_r/I_0 = 0.4474 + 0.00629$[His](μmol L^{-1}) for 10–80 μmol L^{-1} L-his, respectively.

The correlation coefficients were $R^2=0.9868$ and $R^2=0.9966$, respectively. The limit of detection (LOD) was found to be 0.5 μmol L^{-1} using the criterion of three times the standard deviation of the blank signal. The linear range and detection limit of some other methods for the detection of L-his are listed in Table 1 for comparative purpose; it can be seen that our present method offered a comparable detection limit and dynamic range.

3.3. Interference study

To evaluate the selectivity of the proposed detection system, we investigated the fluorescence emission responses of QDs–DA–Ni (II) system to several kinds of amino acids and small biomolecules at the same concentration of L-his, such as arginine (Arg),

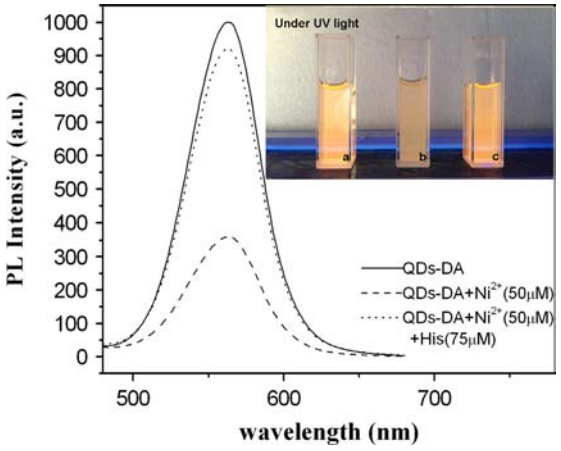

Fig. 2. Photoluminescence emission spectra of QDs–DA. QDs–DA in the presence of 50 μmol L^{-1} Ni^{2+} and QDs–DA mixed with 50 μmol L^{-1} Ni^{2+} and 75 μmol L^{-1} L-histidine shaken thoroughly for 10 min (inset: photo of QDs–DA (a), QDs–DA–Ni (II) system (b) and QDs–DA–Ni (II)-His system (c) under UV light.). (For interpretation of the references to color in this figure, the reader is referred to the web version of this article.)

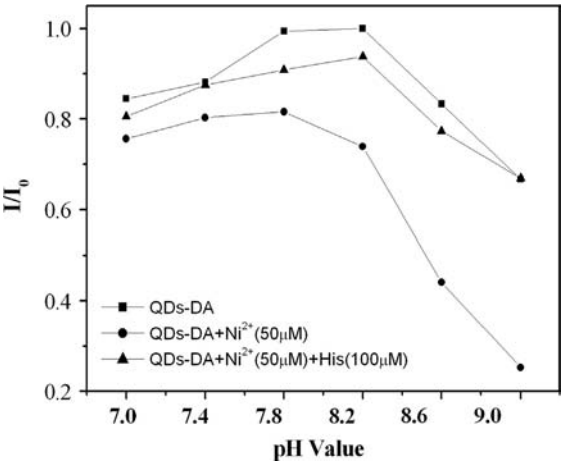

Fig. 3. Effect of pH on the fluorescence quenching of QDs–DA–Ni (II)-His system in the absence and presence of His. I_0 and I represent the photoluminescence intensity of the QDs–DA–Ni (II) system before and after incubation with L-his for 10 min, respectively.

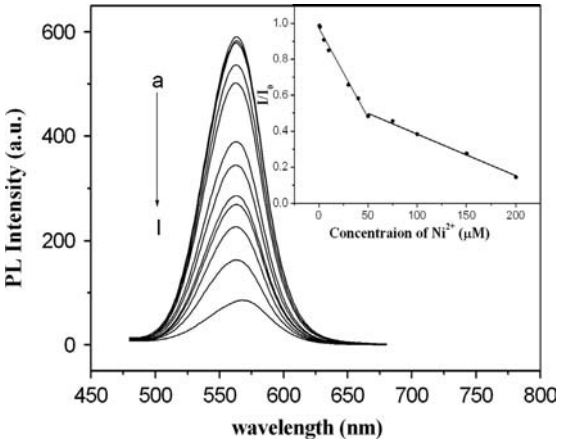

Fig. 4. The photoluminescence intensity change upon the interaction of QDs–DA with different concentrations of Ni^{2+}. The curves a–l represent the concentrations of DA of 0, 0.5, 1.0, 5.0, 10, 20, 35, 50, 75, 100, 150, and 200 μmol L^{-1}, respectively. The inset represents the relationship between I/I_0 value and the concentration of Ni^{2+}; the Ni^{2+} concentration is from 1 μmol L^{-1} to 200 mmol L^{-1}. I_0 and I are the PL intensities in the absence and presence of Ni^{2+}.

tyrosine (Tyr), glycine (Gly), alanine (Ala), phenylalanine (Phe), cysteine (Cys), aspartic acid (Asp), lysine (Lys), beta-cyclodextrin (β-cd), glucose (Glu) and sodium tartarate. The results indicated amino acids and small biomolecules did not produce noticeable effects on the fluorescent emission of QDs–DA–Ni (II) system as compared to that of L-his (Fig. 6). Thus, the dopamine functionalized–CdTe QDs sensor showed good selectivity over other amino acids, especially cysteine. Even though many research results showed both cysteine and L-his have strong binding capacity with divalent metal ions (Cu^{2+}, Hg^{2+}, Zn^{2+}, Cd^{2+}) [12–39], the detection of L-his is more suitable in the presence QDs–DA–Ni (II) system because the imidazole side-chain moiety contained in L-his plays an important role in dissociating Ni^{2+} from the surface of QDs–DA [38].

3.4. Detection of L-histidine in human serum samples

In order to evaluate the feasibility of the proposed method in real sample detection, the developed QDs–DA–Ni (II) fluorescence probe was applied to the detection of L-his in human serum samples. We chose Pauly reagent method [40,41] as a contrast method to detect L-his in human serum samples. The results obtained by standard addition method are shown in Table 2, and the accuracy of the proposed method is evaluated by determining the recoveries of L-his in real samples. The RSD was lower than 3.77 and the recoveries were between 103% and 108%. Compared to the Pauly reagent method, we can see that our developed method is feasible. The above results demonstrated the potential applicability of the QD–DA based fluorescence turn-on probe for the detection of L-his in human serum samples.

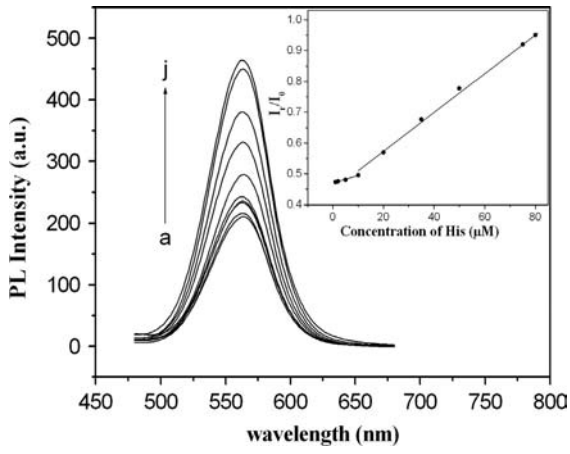

Fig. 5. Photoluminescence intensity change of the QDs–DA–Ni (II) system with different concentrations of L-his. The curves a–j represent the concentrations of L-his of 0, 1.0, 2.0, 5.0, 10, 20, 35, 50, 75, and 80 μmol L^{-1}, respectively. The inset represents the linear relationship between I_r/I_0 value and the concentration of L-his in the solution. I_0 is the PL intensity of QDs–DA in the absence of Ni^{2+} and L-his in solution, and I_r is the PL intensity of QDs–DA–Ni (II) system in the presence of L-his.

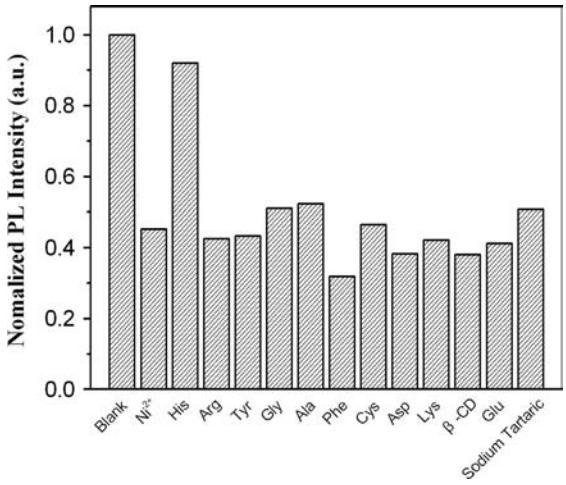

Fig. 6. Response of QDs–DA–Ni (II) system in Tris–HCl buffer (Ni^{2+} 50 μmol L^{-1}, pH 8.6) to the coexisting substance. The concentration of L-his and other coexisting substances is 75 μmol L^{-1}.

Table 2
Results for the detection of L-histidine in human serum samples.

Samples	Added (μmol L^{-1})	Pauly reagent method found (μmol L^{-1})	Our method		
			found (μmol L^{-1})	Recovery (%)	RSD (%, $n=3$)
1	10.00	10.42	10.33 ± 0.34	103.29	3.77
2	20.00	20.00	20.78 ± 0.35	103.91	1.77
3	40.00	41.74	42.96 ± 1.53	107.41	3.82
4	60.00	61.64	60.47 ± 1.83	100.78	3.05
5	80.00	85.34	84.77 ± 0.97	105.96	1.21

The original concentration of L-histidine in human serum samples were subjected to a 50-fold dilution with PBS.

Table 1
Comparison of performance of different methods for L-histidine detection.

Type	Sensing system	Dynamic range (μmol/L)	Selectivity	Detection limit (μmol/L)	Reference
HPLC	Reversed-phase high-performance liquid chromatography	0.01–100	Selective detection of histidine and the isomers of urocanic acid	0.05	[8]
Capillary electrophoresis	Selective isolation of histidine in urine by MAB affinity capillary electrophoresis system	1.0–150	Selective detection of histidine and metabolites (such as histamine)	0.28	[9]
Fluorescence	Lysine-functional silver nanoparticle-based system	5–30	Selective detection of histidine and histidine-tagged proteins	5	[30]
	Ni^{2+}-modulated homocysteine-capped CdTe quantum dots-based photoluminescent sensor	1–30	Being able to separate histidine and imidazole or 2-methylimidazole	0.2	[31]
	Enzymatic recycling cleavage strategy-based amplified fluorescent sensor	2–100	Being able to perform enantio-analysis of histidine	0.2	[32]
	Ni^{2+}-modified gold nanoclusters-based system	0.1–26	Good selectivity for histidine over other natural amino acids	0.03	[33]
	IDA-based colorimetric method for the naked-eye detection and quantification of histidine	2–30	Good selectivity for histidine over other natural amino acids and GSH	0.4	[34]
	Ni^{2+} modified dopamine-functionalized CdTe quantum dots-based photoluminescent sensor	1–80	Good selectivity for for histidine over other natural amino acids	0.3	This work

4. Conclusions

In summary, we successfully synthesized dopamine functionalized–CdTe QDs and developed QDs–DA–Ni (II) system for selective detection of L-his. The fluorescence of QDs–DA was quenched by Ni^{2+} and the strong affinitive behavior between Ni^{2+} and L-his resulted in fluorescence recovery of QDs–DA. A good linear relationship of PL intensity and the concentration of L-his is observed in optimum conditions. Compared with other amino acids and biomolecules, this method is highly selective, label-free and non-toxic. Further more, the proposed fluorescence probes can act as bio-probes for L-his detection in serum which has great potential application in biological systems.

Acknowledgments

This work was financially supported by the National Natural Science Foundation of China (Nos. 21075050 and 21275063).

Appendix A. Supplementary material

Supplementary data associated with this article can be found in the online version at http://dx.doi.org/10.1016/j.talanta.2014.02.060.

References

[1] T.E. Creighton, Encyclopedia of Molecular Biology, 2, 1147.
[2] C. Guo Nan, W. Xiao Ping, D. Jian Ping, C. Hong Qing, Talanta 49 (1999) 319–330.
[3] Y. Kusakari, S. Nishikawa, S. Ishiguro, M. Tamai, Curr. Eye Res. 16 (1997) 600–604.
[4] N.M. VanGelder, F.B.M. Roy, S. Paris, A. Barbeau, Curr. Top. Nutr. Dis. 16 (1987) 271.
[5] M.L. Rao, H. Stefan, C. Scheid, A.D.S. Kuttler, W. Froscher, Epilepsia 34 (1993) 347–354.
[6] M. Watanabe, M.E. Suliman, A.R. Qureshi, E. Garcia-Lopez, P. Bárány, O. Heimbürger, P. Stenvinkel, B. Lindholm, Am. J. Clin. Nutr. 87 (2008) 1860–1866.
[7] K. Hermann, D. Abeck, J. Chromatogr. B 750 (2001) 71–80.
[8] M. Takahashi, T. Tezuka, J. Chromatogr. B 688 (1997) 197–203.
[9] J. Meng, W. Zhang, C.-X. Cao, L.-Y. Fan, J. Wu, Q.-L. Wang, Analyst 135 (2010) 1592–1599.
[10] M. Shahlaei, M.B. Gholivand, A. Pourhossein, Electroanalysis 21 (2009) 2499–2502.
[11] T. Natsume, H. Nakayama, Ö. Jansson, T. Isobe, K. Takio, K. Mikoshiba, Anal. Chem. 72 (2000) 4193–4198.
[12] F. Pu, Z. Huang, J. Ren, X. Qu, Anal. Chem. 82 (2010) 8211–8216.
[13] M. Shojaei, A. Mirmohseni, M. Farbodi, Anal. Bioanal. Chem. 391 (2008) 2875–2880.
[14] U. Resch-Genger, M. Grabolle, S. Cavaliere-Jaricot, R. Nitschke, T. Nann, Nat. Methods 5 (2008) 763–775.
[15] J.L. Nadeau, S.J. Clarke, C.A. Hollmann, D.M. Bahcheli, R.A. Khatchadourian, A. Bachir, P. Wiseman, Biomedical Optics (BiOS), in: Marek Osinski, Thomas M. Jovin, Kenji Yamamoto (Eds.), International Society for Optics and Photonics, San Jose, CA 2007, (64480M-64480M-64412).
[16] M. Sunbul, M. Yen, Y. Zou, J. Yin, Chem. Commun. (2008) 5927–5929.
[17] M. Frasco, N. Chaniotakis, Anal. Bioanal. Chem. 396 (2010) 229–240.
[18] S. Lai, X. Chang, C. Fu, Microchim. Acta 165 (2009) 39–44.
[19] H. Li, Y. Zhang, X. Wang, Z. Gao, Microchim. Acta 160 (2008) 119–123.
[20] R. Baron, M. Zayats, I. Willner, Anal. Chem. 77 (2005) 1566–1571.
[21] A. Brown, S. Gershon, J. Neural Trans. 91 (1993) 75–109.
[22] S.J. Clarke, C.A. Hollmann, Z. Zhang, D. Suffern, S.E. Bradforth, N.M. Dimitrijevic, W.G. Minarik, J.L. Nadeau, Nat. Mater. 5 (2006) 409–417.
[23] R. Khatchadourian, A. Bachir, S.J. Clarke, C.D. Heyes, P.W. Wiseman, J.L. Nadeau, J. Biomed. Biotechnol. 2007 (2007) 1–10.
[24] D.R. Cooper, D. Suffern, L. Carlini, S.J. Clarke, R. Parbhoo, S.E. Bradforth, J.L. Nadeau, Phys. Chem. Chem. Phys. 11 (2009) 4298.
[25] K.A. Fraser, M.M. Harding, J. Chem. Soc. A (1967) 415–420.
[26] Y. Liu, Y. Li, Z.-Q. Wu, X.-P. Yan, Talanta 79 (2009) 1464–1471.
[27] J.-W. Liu, T. Yang, L.-Y. Ma, X.-W. Chen, J.-H. Wang, Nanotechnology 24 (2013) 505704.
[28] J.-W. Liu, T. Yang, S. Chen, X.-W. Chen, J.-H. Wang, J. Mater. Chem. B 1 (2013) 810–818.
[29] C. Wang, Q. Ma, X. Su, J. Nanosci. Nanotechnol. 8 (2008) 4408–4414.
[30] H. Huang, Y. Gao, F. Shi, G. Wang, S.M. Shah, X. Su, Analyst 137 (2012) 1481–1486.
[31] S. Liu, F. Shi, X. Zhao, L. Chen, X. Su, Biosens. Bioelectron. 47 (2013) 379–384.
[32] M. Masoud, T. Kassem, M. Shaker, A. Ali, J. Therm. Anal. Calorimetry 84 (2006) 549–555.
[33] J. Guan, L. Jiang, J. Li, W. Yang, J. Phys. Chem. C 112 (2008) 3267–3271.
[34] D.R. Bae, W.S. Han, J.M. Lim, S. Kang, J.Y. Lee, D. Kang, J.H. Jung, Langmuir 26 (2009) 2181–2185.
[35] P. Wu, X.-P. Yan, Biosens. Bioelectron. 26 (2010) 485–490.
[36] L.-D. Li, Z.-B. Chen, H.-T. Zhao, L. Guo, Biosens. Bioelectron. 26 (2011) 2781–2785.
[37] Y. He, X. Wang, J. Zhu, S. Zhong, G. Song, Analyst 137 (2012) 4005.
[38] S.-K. Sun, K.-X. Tu, X.-P. Yan, Analyst 137 (2012) 2124–2128.
[39] M. Belcastro, T. Marino, N. Russo, M. Toscano, J. Mass Spectrometry 40 (2005) 300–306.
[40] M. Tomita, M. Irie, T. Ukita, Biochemistry 8 (1969) 5149–5160.
[41] M. Sato, Z. Tao, K. Shiozaki, T. Nakano, T. Yamaguchi, T. Yokoyama, N. Kan-No, E. Nagahisa, Fisheries Science 72 (2006) 889–892.